Geosci. Model Dev. Discuss., 7, C132–C138, 2014
www.geosci-model-dev-discuss.net/7/C132/2014/

Open Access
Geoscientific Model Development

Interactive comment on "Simulations of direct and reflected waves trajectories for in situ GNSS-R experiments" by N. Roussel et al.

F. Nievinski (Referee)
fgnievinski@gmail.com
Received and published: 17 March 2014

➔ Following the main point of the reviewer, many new calculations were done, and the text of the article was supplemented by new results. As attachment you will find the modified version of the article (RousselN_new.pdf) and also a pdf file where modifications and corrections between the two versions of the article are highlighted (RousselN_corrections.pdf).

GENERAL COMMENTS

The article is well written and illustrated, and tackles a topic of active development in the literature. On the other hand, I have contentions concerning the breadth versus depth in the subject coverage. The submission tries to tackle three separate issues in the simulation of GNSS reflection trajectories: - large-scale surface model - use of a detailed digital elevation model (DEM) - tropospheric refraction I believe any of these three topics individually would suffice, were it dealt with in a thorough and conclusive manner, which unfortunately does not seem to be the case.

➔ Your point is relevant and we agree with the fact that we must be careful about the breadth versus depth in the subject coverage. The main purpose of the development presented here was to have an easy-to-use simulator able to give quickly precise coordinates of specular reflection points, with a known receiver and a given satellite constellation, which explains why different algorithms have been implemented and compared: the final aim being to choose, for given initial conditions, the relevant algorithm able to give well-enough results given the wanted accuracy.

Starting with the surface models, it fails to cover the simplest one, that of a planar horizontal surface (is the curvature of the Earth significant at the lighthouse scenario?);

➔ A new subsection *3.1. Local plane reflection approximation* was added in the new version of the article (page 4, line 321), and the results of such an approximation were compared to the sphere approximation (chosen as a reference). → see tables of results at the end of this document.

3.1 Local plane reflection approximation

Let us consider the projection of the receiver R0 on an osculating sphere approximation (figure 3). We define the local plane P as the plane tangent to the sphere at R0. Let T0 be the projection of the satellite on P and R' the symmetry of R0 relative to P. We look for the positions of the specular reflection points on P. Considering the Thales theorem in the triangles R' S R0 and S T T0, we have (see figure 3):

$$\frac{X_S}{X_{TO} - x_S} = \frac{h}{H}$$

And so:

$$X_S = \frac{hX_{T0}}{X_{T0} + h}$$

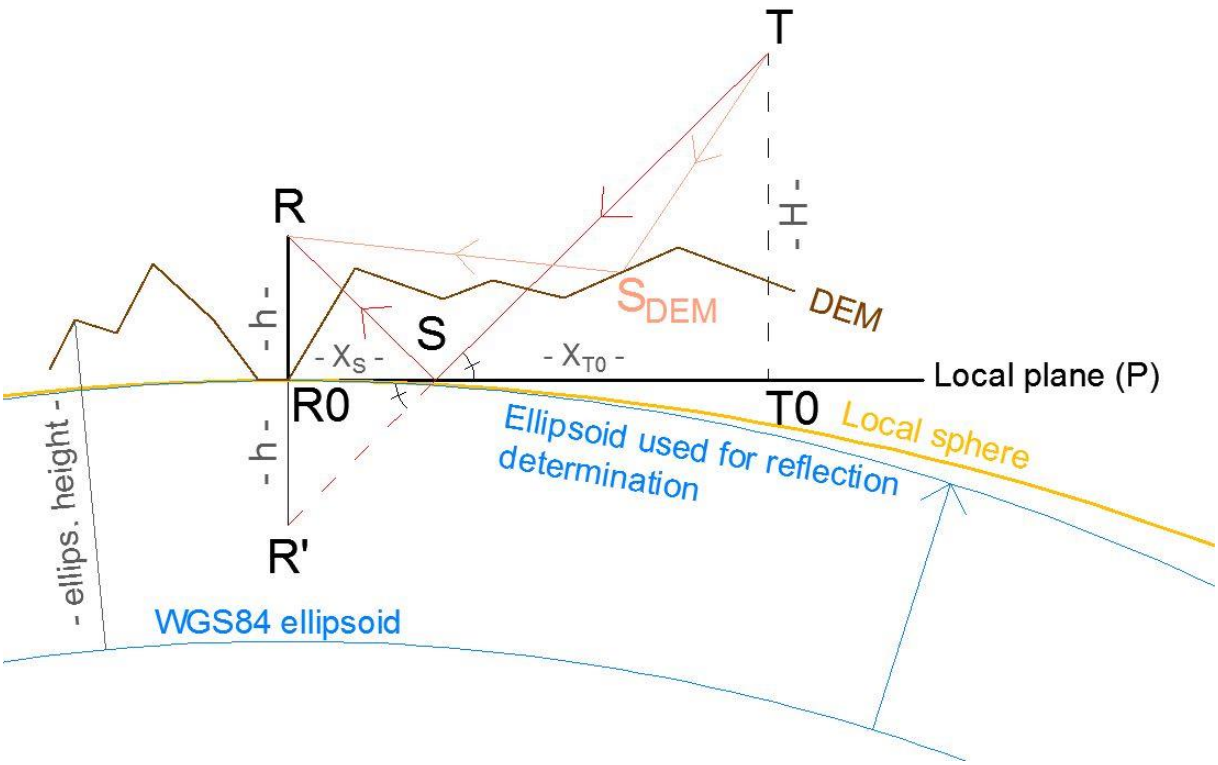

Figure 3. Determination of the specular reflection point in a local plane approximation and local difference with the sphere and ellipsoid approximations and DEM integration.
S: specular reflection point position. R: receiver position. T: transmitter/satellite position. h: height of the receiver above the ground surface.

The spherical model needs to distinguish between a geocentric sphere and an osculating sphere (also: how does the iterative procedure compares closed-form solutions reported in the literature?); the ellipsoidal model lacks further development towards a closed-form solution (after all, the ray/ellipsoid intersection has well-known solution in the computer-graphics literature);

- ➔ The spherical model used is osculating, with the Gaussian radius of curvature.
- ➔ The spherical model algorithm (analytical with an iterative procedure based on the Newton method to determine the roots of a fourth order polynomial) is compared to the ellipsoid algorithm (in the new subsection 4.2), which is a pure iterative procedure (close to the algorithm presented in (Kostelechy et al 2005)). By putting the semi-major and –minor axis of the ellipsoid equal to the radius of the sphere, differences are sub-millimetric. See the new subsection 4.2 Validation of the surface models (page 7, line 611).

4.2 Validation of the surface models

Simulations have been performed in the case of the Geneva Lake shore, for a 24-hour experiment, on the 4th October 2012.

4.2.1 Cross-validation between sphere and ellipsoid approximations

Local sphere and ellipsoid approximation algorithms have been compared by putting the ellipsoid semi-major and minor axis equal to the sphere radius. Planimetric and altimetric differences between both are below 6.10^{-5} m for a receiver height above reflecting surface between 5 and 300 m and are then negligible. The two algorithms we compare are totally different: the first is analytical and the second is based on a iterative scheme and both results are very similar, which confirms their validity.

- ➔ See also the new paragraph added to subsection 3.2 Local sphere reflection approximation, page 4 line 332.

J. Kostelecky and C. Wagner already suggested an algorithm to retrieve the specular reflection point positions by approximating the Earth as a sphere in (Kostelecky J. et al., 2005; Wagner C., Klokocnik J., 2003). Their algorithm is based on an optimized iterative scheme which is equivalent to make the position of a fictive specular point vary until verifying the first law of Snell-Descartes. A similar approach will be used in this paper in the subsection 3.3 with the ellipsoid approximation. Here we chose to adopt a more analytical algorithm, first proposed by (Helm A., 2008). In order to validate this algorithm, comparisons between it and the iterative one developed for the ellipsoid approach will be done, by setting the minor and major axis of the ellipsoid equal to the sphere radius (see part 4.2.1).

- ➔ The ellipsoid approximation algorithm has been slightly modified by adopting a dichotomous process in order to increase the speed of convergence. See subsection 3.3 Ellipsoid reflection approximation page 5, line 406.

3.3 Ellipsoid reflection approximation

By knowing the locations of the transmitter and the receiver on the local ellipsoid included in the plane defined by the centre of the Earth, the receiver and the transmitter, let us consider the two normalized anti-incident r_t and scattering r_r vectors. When the Snell-Descartes law is verified, the sum of the two vectors (bisecting vector dr) coincides with the local vertical r_s (figure 5). The determination of the

location of the reflection point is based on iterative process proposed earlier by (Gleason S. et al. , 2009), and enhanced with a dichotomy process. Let us consider three points on the ellipsoid:
– S1 the projection of the receiver on the ellipsoid
– S3 the projection of the transmitter on the ellipsoid
– S2 the projection of the middle of [S1S3] on the ellipsoid

We calculate dr, the correction in direction, for each of the three points:

$$dr(t) = \frac{r_s(t) - r_r(t)}{\|r_s(t) - r_r(t)\|} + \frac{r_s(t) - r_t(t)}{\|r_s(t) - r_t(t)\|} \qquad (19)$$

We consider then the direction of the correction dr. If the correction is in the satellite direction, the sign is considered as positive, and negative if the correction is in the receiver direction. If the signs of dr_{S1} *and* dr_{S2} *are different, it means that the specular reflection point is located between S1 and S2.We thus consider a new iteration with S1 = S1, S3 = S2 and S2 the projection on the ellipsoid of the middle of the new S1 and S3 points. We thus eliminate the part between the initial S2 and S3 points. Else if the signs of* dr_{S2} *and* dr_{S3} *are different, we consider a new iteration with S1 = S2 and S3 = S3 (and S2 the projection on the ellipsoid of the middle of the new S1 and S3 points). The iterative process stops when the difference between incident and reflected angle (with respect to the local vertical) is close to zero with a fixed tolerance of 1e-7°.*

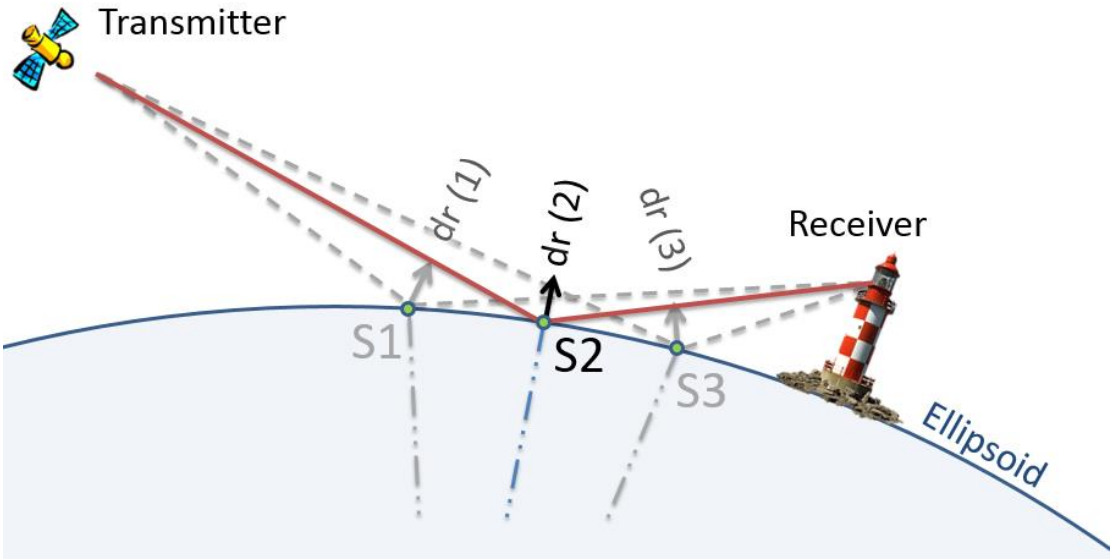

Fig. 5. Local ellipsoid approximation.
S2: specular reflection point position. S1, S3: temporary positions of the specular reflection point before convergence. Let dr be the sum of the normalized anti-incident and scattering vector (i.e. the bisecting vector). In the specular reflection point position, dr is colinear with the local vertical. We apply a dichotomous process until having this condition verified.

Finally, there is little verification and validation reported here – authors could use the simpler models to check on the more complicated ones, forcing the latter to artificially degenerate into the former (e.g., an ellipsoid with equal major and minor axes, a sphere with near-infinite radius, etc.)

➔ A new subsection 4.2 *Validation of the surface models* was added in the new version of the article (page 7, line 611), with a cross-validation between sphere and ellipsoid approximations (sub-millimetric differences) and a cross-validation between ellipsoid approximation and DEM integration (centimetric differences).

4.2 Validation of the surface models

Simulations have been performed in the case of the Geneva Lake shore, for a 24-hour experiment, on the 4th October 2012.

4.2.1 Cross-validation between sphere and ellipsoid approximations

Local sphere and ellipsoid approximation algorithms have been compared by putting the ellipsoid semi-major and minor axis equal to the sphere radius. Planimetric and altimetric differences between both are below 6.10^{-5} m for a receiver height above reflecting surface between 5 and 300 m and are then negligible. The two algorithms we compare are totally different: the first is analytical and the second is based on a iterative scheme and both results are very similar, which confirms their validity.

4.2.2 Cross-validation between ellipsoid approximation and DEM integration

The algorithm integrating a DEM has been compared to the ellipsoid approximation algorithm by putting a flat DEM as input (i.e. a DEM with orthometric altitude equal to the geoid undulation). Results for satellite elevation angles above 5° are presented in table 1. As we can see in table 1, planimetric and altimetric mean differences are subcentimetric for a 5 and 50 m receiver height and centimetric for a 300 m receiver height. However, some punctual planimetric differences reach 70 cm in the worst conditions (reflection occurring at 3408 m from the receiver corresponding to a satellite with a low elevation angle), which can be explained with the chosen tolerance parameters but mainly because due to the DEM resolution, the algorithm taking a DEM into account approximating the ellipsoid as a broken straight line, causing inaccuracies. For a 50 m receiver height, planimetric differences are below 10 cm (reflections occurring until 573 meters from the receiver). With regards to the altimetric differences, even for reflections occurring far from the receiver, the differences are negligible (submillimetric).

Table 1. Cross-validation between ellipsoid approximation and DEM integration

		Receiver height (m)		
		5	50	300
Distance to the specular reflection point with respect to the receiver: arc length (m)	Mean	13	122	730
	Maximum	58	573	3408
Position differences (m) (planimetric / altimetric)	Mean	**0.007/0**	**0.008/0**	**0.04/0**
	Maximum	0.1/0	0.1/0	0.7/0

The use of the DEM consists of two main parts: visibility masking and surface slope variations. The first part seems reasonable and indeed is useful in the scenarios demonstrated; it does not seem to address, though, the issue of visibility of the satellite and of the receiver, both from the specular point (only the visibility of the satellite from the receiver).

- ➔ It was maybe not explained sufficiently clearly in the first version of the article, but the issue of visibility of the satellite and of the receiver from the specular point is addressed. The main steps of the algorithm are :
  - Check the visibility of the satellite from the receiver
  - If the satellite is visible, we find the location of the specular reflection point on the DEM.
  - Once the position of the specular reflection point is found, we check its visibility from the receiver and the satellite.

  See subsection 3.4 Ellipsoid reflection approximation combined with a DEM page 6, line 440.

3.4 Ellipsoid reflection approximation combined with a DEM

The two first approaches presented above are well adapted in the case of an isolated receiver, located on the top of a light house, for instance. In most of the cases, the receiver is located on a cliff, a sand dune, or a building overhanging the sea surface or a lake. It can however be really appropriate and necessary to incorporate a Digital Elevation Model (DEM) into the simulations, in order not to only take the mask effects (e.g., a mountain occulting a GNSS satellite) into account, but also to get more accurate and realistic positions of specular reflection points. The method we propose here consists of three steps later detailed in subsections 3.4.1, 3.4.2 and 3.4.3.

1. A "visibility" determination approach to determine if the receiver is in sight of each GNSS satellite.
2. A determination of the specular reflection point position.
3. A "visibility" determination approach to determine if the determined specular point is sight from both receiver and satellite.

The second part is more contentious: I do not think the heuristics employed in its derivation (e.g., reflection assumed to occur along a planar cross section, Snell law being applied with no due consideration for the DEM resolution vis-a-vis the Fresnel zone area) should be trusted before they are proven correct upon comparison to a more rigorous formulation, such as geometrical-optics ray-tracing or physical-optics integration.

➔ Indeed, the algorithm we proposed was based on the assumption that reflections occur along a planar cross section, which is not relevant when integrating a DEM (as you commented it in the annotated PDF). That is why we adopted a new approach as presented in this new version of the article. We only consider the reflections occurring in the plane containing the receiver, the satellite and the center of the Earth. It's true, that when we take a DEM into account, reflections can also occur out of this plane, but we only consider those contained in the plane: first because considering all the potential reflections would take a huge calculation time, and secondly because I consider the DEM integration as a way to have positions closer to reality w.r.t the sphere, plane or ellipsoid approximations, i.e. as a correction to the other algorithms, where reflections occur only within the plane.

See page 4, line 312:

In the plane, sphere and ellipsoid approximations, the specular reflection point of a given satellite is contained within the plane defined by the satellite, the receiver and the center of the Earth. With regards to the DEM integration, reflection can occur everywhere. In order to be able to compare the specular reflection point positions obtained by integrating a DEM, and to simplify the problem, we will only consider the reflections occurring within the plane, even while integrating a DEM.

And see subsection 3.4 Ellipsoid reflection approximation combined with a DEM, page 6, line 440.

3.4 Ellipsoid reflection approximation combined with a DEM

The two first approaches presented above are well adapted in the case of an isolated receiver, located on the top of a light house, for instance. In most of the cases, the receiver is located on a cliff, a sand dune, or a building overhanging the sea surface or a lake. It can however be really appropriate and necessary to incorporate a Digital Elevation Model (DEM) into the simulations, in order not to only take the mask effects (e.g., a mountain occulting a GNSS satellite) into account, but also to get more accurate and realistic positions of specular reflection points. The method we propose here consists of three steps later detailed in subsections 3.4.1, 3.4.2 and 3.4.3.

1. A "visibility" determination approach to determine if the receiver is in sight of each GNSS satellite.

2. A determination of the specular reflection point position.

3. A "visibility" determination approach to determine if the determined specular point is in plane of sight receiver/satellite.

We have to keep in mind that a DEM gives altitudes above a reference geoid. For consistency purpose, the positions of the receiver and the transmitter, and the DEM grid points have all to be in the same reference system. So it is absolutely mandatory to convert the altitudes of the DEM grid points into ellipsoidal heights by adding the geoid undulation. To do so, a global grid from the EGM96 geoid undulation model with respect to the WGS84 ellipsoid was removed from SRTM DEM grid points.

3.4.1 Visibility of the GNSS satellite from the receiver

This algorithm aims to determine the presence of mask between the receiver and the satellite. The visibility of the satellite and of the receiver, both from the specular point will be checked once the potential specular point position will be found.
Let R, S, and T be the locations of the receiver, the specular point and the satellite/transmitter on the ellipsoid. We interpolate the ellipsoidal heights along the path [TSR] with a step equal to the DEM resolution, with a bivariate cubic or bilinear interpolation. Cubic interpolation is used when the gradient is big, linear interpolation otherwise. Tests show millimetric differences between cubic and linear interpolation for flat zones but can reach one meter for mountainous areas. We thus obtain a topographic profile from R to T. For each segment of this topographic profile, we check if it intersects the path [TR]. If it does, it means that the satellite is not visible from the receiver. If not, we check the next topographic segment, until reaching the end of the path (i.e. T).

3.4.2 Position of the specular point

Once the satellite visibility from the receiver is confirmed, the next step consists in determining the location of the specular reflection point S along the broken line defined as in subsection 3.4.1. In order to simplify the process, we only consider the specular points located into the plane formed by the satellite, the receiver and the center of the Earth. The algorithm is similar to the one used for the ellipsoid approximation and is based on a dichotomous iterative process. The segments formed by the points of the 2D DEM (see figure 6) are all considered susceptible to contain a specular reflection point. For each of this segment, we check the sign of the correction to apply for the two extremities of the segment with the same principle that for the ellipsoid approximation (see subsection 3.3), but with a local vertical component defined as the normal of the considered segment. If the signs are equal, no reflection is possible on this segment. Otherwise, we apply the dichotomous iterative method presented in subsection 3.3 until convergence with respect to the tolerance parameter (fixed to 1e-7°).

3.4.3 Visibility of the determined specular reflection point from the satellite and the receiver

Once the position of the specular reflection point is determined, we check if it is visible from the satellite and the receiver thanks to the algorithm presented in subsection 3.4.1.

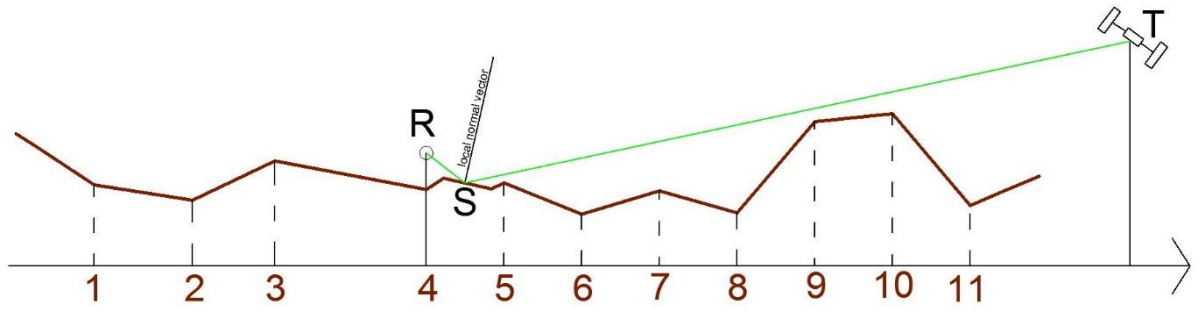

Fig. 6. Determination of the specular reflection point integrating a DEM
S: specular reflection point position. R: receiver position. T: transmitter/satellite position. A dichotomous process is applied for each topographic segment of the DEM to find if there is a point where the bisecting angle (equal to the sum of the anti-incident and scattering vectors) is colinear with the local normal vector.

The treatment of tropospheric refraction must be disentangled. On the one hand, there is the angular or directional refraction, which changes the signal direction of arrival (primarily the elevation angle, secondarily also its azimuth). On the other hand, there is the refraction range or delay. It remains unclear the relative contribution of the two types with varying satellite direction – it'd seem that angular refraction is greatest near grazing incidence while ranging refraction seems greatest near normal incidence (considering reflected minus direct paths). The latter effect would need a zenith delay model, which is not normally part of a mapping as the AMF employed. Besides these main issues, there are secondary ones, such as the need for a bulky numerical weather model vs. a leaner climatology, and whether or not azimuthal asymmetries are significant. These issues are all touched in the article though only in an inconclusive manner.

➔ The AMF tropospheric corrections used in this study are a final product computed following (Gegout P. et al, 2011) and provided by GRGS (Groupe de Rercherche en Géodésie Spatiale). They are not properly "mapping functions" as used by the community. AMF are constituted in two parts:

- a scale factor which has the same role in AMF than the zenithal delay in classical mapping functions;
- a successive fraction to rely the scale factor and the tropospheric delay at any elevation and azimuth angles.

See:

Gegout P., Biancale R., Soudarin L.: Adaptive Mapping Functions to the azimuthal anisotropy of the neutral atmosphere. J. Geodesy., 85, 661-667, 2011.

➔ Answer to your specific comment about the convergence process p 1018 – 11.

It appears that I must not have been clear enough about my method. Here are the main steps:

- I consider the position of the specular reflection point without any correction of the tropospheric errors.
- I calculate the corrections to apply to this specular point knowing the incident and reflecting angle corresponding to the considered reflection point. I obtain a corrected incident angle. Figure 7 in the paper shows the correction to apply as a function of the elevation angle.
- With the corrected incident angle, I calculate a corrected position of the specular point (making the reflecting angle equal to this corrected incident angle).
- With the new position of the specular point, I do a second iteration calculating the corrections to apply to the new incident angle. These new corrections are really small as plotted in the following figure (which is the same than the figure 7, but for the second iteration):

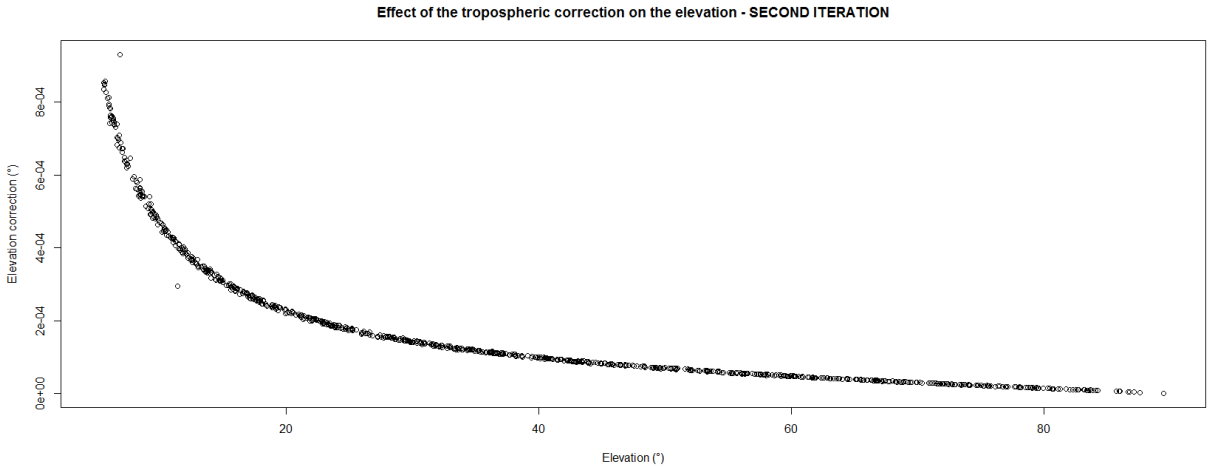

- More iterations are useless because the corrections to apply becomes negligible, but only one iteration is not enough, because the first corrections we calculate are based on a point whose position is "far" from the one after integrating the troposphere influence.

➔ Subsection 2.5 Adaptive Mapping Function, page 3, line 217 has been slightly modified to make it clearer:

2.5 Adaptive Mapping Functions

The neutral atmosphere bends the propagation path of the GNSS signal and retards the speed of propagation. The range between the satellite and the tracking site is neither the geometric distance nor the length of the propagation path, but the radio range of the propagation path (Marini J.W. , 1972).
For GNSS-R measurements, the tropospheric effects induced by the neutral part of the atmosphere are an important source of error. Indeed, GNSS-R measurements are often done at low elevation angle where the bending effects are maximal. Accurate models have to be used to mitigate signal speed decrease and path bending. It is commonly accepted to model tropospheric delays by calculating the zenith tropospheric delay and obtaining the slant tropospheric delays with a mapping function. New mapping functions have been developed in the 2000's (Boehm J. et al, 2006; Niell A., 2001) and significantly improve the geodetic positioning. Although modern mapping functions like VMF1 (Boehm J. et al , 2006b) and GPT2/VMF1 (Lagler K. et al. , 2013) are derived from Numerical Weather Models (NWM), most of these mapping functions ignore the azimuth dependency which is usually introduced by two horizontal gradient parameters - in north-south and east-west directions – estimated directly from observations (Chen G. et al. , 1997). More recently, the use of ray-traced delays through NWM directly at observation level has shown an improvement on geodetic results (Hobiger T. et al , 2008; Nafisi V. et al , 2012; Zus F., et al , 2012). The Adaptive Mapping Functions (AMF) are designed to fit the most information available in NWM – especially the azimuth dependency - preserving the classical mapping function strategy. AMF are thus used to approximate thousands of atmospheric ray-traced delays using a few tens of coefficients with millimetre accuracy at low elevation (Gegout P. et al. , 2011).
AMF have a classical form with terms which are function of the elevation. But, they also include coefficients which depend on the azimuth to represent the azimuthal dependency of ray-traced delays. In addition, AMF are suitable to adapt to complex weather by changing the truncation of the successive fractions. Therefore, the AMF are especially suited to correct propagation of low elevation GNSS-R signals. In our study we use AMF directly provided by GRGS (Groupe de Recherche en G´eod´esie Spatiale) and computed following (Gegout P. et al., 2011).

➔ And also subsection 3.5 Tropospheric corrections, page 6, line 515

3.5 Tropospheric corrections

In order to correct the anisotropy of propagation of radio waves used by the GNSS satellites, we use AMF calculated from the 3-hourly delayed cut-off in model levels computed by the ECMWF (European Centre for Medium Range Weather Forecasts). AMF tropospheric corrections were computed following

(Gegout P. et al., 2011) and provided by GRGS for this study. Given the geometric specificities of the specular reflection point, two paths have to be checked for propagation error: the first one from the satellite to the surface, and the second from the surface to the receiver. The main steps of the process are the following:

1 We consider the position of the specular reflection point without any correction of the tropospheric errors;

2 We calculate the corrections to apply to this specular point knowing the incident and reflecting angle corresponding to the considered reflection point. We thus obtain a corrected incident angle. Figure 7 shows the correction to apply as a function of the elevation angle;

3 With the corrected incident angle, a corrected position of the specular point is calculated, making the reflecting angle being equal to the corrected incident angle;

4 With the new position of the specular point and to reach a better accuracy of the point position, a second iteration is done calculating the corrections to apply to this new incident angle.

3.5.1 Correction of the satellite-surface path

First and foremost, we solve the parallax problem for the wave emitted by a known GNSS satellite. At first sight, we consider the position of the specular reflection point calculated without any tropospheric correction, given by the algorithm approximating the Earth's shape as a sphere given in paragraph 3.2.We use here AMF calculated from the projection of the receiver on the surface, considering that the AMF planimetric variations are negligible for ground-based observations (i.e. we consider that we can use the same AMF for every specular reflection points, which is valid only if the specular reflection points are less than few tens of kilometres from the receiver and that the specular points lie on an equal height surface). We thus obtain the corrected incident angle of the incident wave. Considering the law of Snell-Descartes, the reflecting angle must be equal to the corrected incident angle, for the specular reflection point position.

3.5.2 Correction of the surface-receiver path

The aim here is to adjust the surface-receiver path to accommodate for the consequences of angular refraction. With the corrected reflection angle, we can deduce the corrected geometric distance between the reflection point and the receiver, using this time AMF calculated from the receiver, assuming that the AMF altimetric variations are non-negligible (i.e. the part of the troposphere corresponding to the receiver height will have a non-negligible impact on the AMF). Considering the corrected geometric distance between the reflection point and the receiver, the corrected position of the reflection point is obviously determined. It is indeed obtained by intersection between a circle whose radius is equal to the correct geometric distance, and the surface of the Earth assimilated as a sphere, an ellipsoid, or with a DEM, depending on which approximation of the Earth is taken into account. We iterate the whole process a second time to reach a better accuracy of the reflection point position. In fact, the first corrections were not perfectly exact since calculated from an initially false reflection point position, and the second iteration brings the point closer to the correct position. More iterations are useless (corrections to apply are no significant). Figure 7 shows an example of elevation corrections to apply as a function of the satellite elevations. This figure has been computed from simulations done on a receiver placed on the Geneva Lake shore (46°24'30N" ; 6°43'6"E ; 471m): see subsection 4.1 page 7.

For the above-mentioned reasons, I find the coverage of the subject to be too broad at the risk of being shallow; I'd prefer to see a narrower scope and deeper treatment. May I suggest authors focus on the surface model part, as it the one requiring the least modifications to produce an acceptable article. There is an opportunity for the authors to offer guidelines to fellow scientists concerning when it is no longer acceptable to employ the simplified models. Yet, to reap these benefits, the reporting of results also should be improved. In addition to the observation conditions (essentially satellite elevation angle and receiver height above the surface), also the reflection characteristics need clarification: instead of a combined three-dimensional position, please report vertical position separately from horizontal position (Cartesian or geodesic arc-length), as well as slant distance or propagation range. It'd be useful to emphasize whether these systematic errors translate into, e.g., over- or under-estimated reflector height, etc.

➔ We took your comments into account in the new version of the paper, mainly in the last part: 4.4 Results and in the conclusion, but also in the abstract and in the body of the article.

Influence of the receiver height above the reflecting surface

It appears that both planimetric and altimetric differences between the method used increase with the receiver height above the reflecting surface. This is explainable by the fact that the higher the receiver is, the farther the reflection points will be from the receiver, and the bigger the impact of the Earth approximation will be. For a 5-meter receiver height, reflection occurs until approximately 60 meters from the receiver, whereas for a 300-meter receiver height, it occurs until 3400 meters (6700 m when integrating the DEM). It means that, in the second case, reflections occur in the mountains in the South of the receiver hence big differences between the sphere algorithm and the algorithm taking the DEM into account. For a 5 m receiver height above the reflecting surface and considering satellites with elevation angles above 5°, mean planimetric (resp. altimetric) differences are below 11 cm (resp. 2 cm) between the local sphere and ellipsoid approximation and are negligible between the sphere and plane approximations. With a 300 m receiver height above the reflecting surface, mean planimetric (resp. altimetric) differences reach 7.70 m (resp. 1.19 m) between the local sphere and ellipsoid approximation and 2.1 m (resp. 8 cm) between the local sphere and plane approximations.

Influence of the satellite elevation angle

Secondly, by plotting the differences as functions of the satellite elevation angles, we can observe that the lapses between the different algorithms vary in an inversely proportional way than the satellite elevation angle (and so, proportionally to the point distance from the receiver). That is why we re-ran the simulations, putting a more restrictive mask of visibility, tolerating only satellites whose elevation angle is between 10° and 90°. Tables 5, 6, 7 show results we obtain by applying such a mask. The lower the satellite elevation angle is, the farther the specular reflection points from the receiver and the bigger the impact of the Earth approximation is. The choice of the algorithm used to perform the simulations becomes thus really important for the farthest reflection points (i.e for low satellite elevation angles, and high receiver height above the reflecting surface). For example, mean planimetric (resp. altimetric) differences between the local sphere and ellipsoid approximation with a 50 m receiver height are about 1.20 m (resp. 19 cm) considering satellites with elevation angles above 5° and are about 64 cm (resp. 13 cm) considering only satellites with elevation angles above 10°. Mean planimetric differences between the local sphere and plane approximation with a 50 m receiver height are about 6 cm considering the satellites with elevation angles above 5° and are about 2 cm considering only the satellites with elevation angles above 10°. Altimetric differences are negligible in both cases.

Influence of the DEM integration

Integrating a DEM has deleted 245 specular reflection points out of the 905 points determined during 24 hours the 4th of October 2012 with the sphere approximation algorithm (figure 15a). These 245 points came from a wave emitted by a satellite hidden by a mountain located in the south part of the area. In the north part, any reflection point is valid when taking a DEM into account, because in that direction,

the relief is flat over the Geneva Lake, and so, satellites are all visible and reflections are possible (figure 15b). Moreover, the points positions have been rectified while taking a DEM into account, since the others algorithms consider that reflections occur (in first approximation) in a plane around the projection of the receiver and without integrating the problem of the presence of relief.

Comparison between algorithms

For a 5-meter receiver height, and for satellite elevations greater than 10°, the mean planimetric difference (resp. altimetric) between the ellipsoid and the sphere algorithm is equal to 5 cm (resp. 1 cm) whereas for a 300-meter receiver height it is equal to 3.81 m (resp. 75 cm). The approximation done by considering the Earth as a sphere or as an ellipsoid does not really affect the precision of the specular reflection point determination when reflection does not occur too far from the receiver (maximum equal to 48 cm (resp. 9 cm) for a distance inferior to 28 m) i.e. for low receiver height and high satellite elevation. When reflections occur far from the receiver, the choice of the approximation begins to be important. Concerning the algorithm taking the DEM into account, the differences obtained with respect to the sphere or ellipsoid algorithms are quite big even if the specular reflection point is close enough from the receiver. For instance, the mean difference between the sphere algorithm and the one integrating the DEM is bigger than 2.3 m (resp. 9.22 m) for a 5-meter receiver height, and bigger than 92 m (resp. 37 m) for a 300-meter receiver height, and with satellite elevation angle above 5°.

[…]

5 Conclusions

[…]

- *the DEM integration is really important for mountainous areas: planimetric differences as arc length (resp. altimetric differences as ellipsoid height) can reach 5.4 km (resp. 1.0 km) for a 300-meter receiver height, considering satellite with elevation angle greater than 10°.*
- *differences between sphere and ellipsoid approximation are negligible for specular reflection points close from the receiver (closer than 40-50 meters) i.e. small receiver height and/or high satellites elevations. For instance, planimetric differences (resp. altimetric) are smaller than 50 cm (resp. 10 cm) for a 5-meter receiver-height, considering satellites with elevation angle greater than 10°.*

[…]

SPECIFIC COMMENTS

Here I highlight some of the intermediary-level issues; please see comments on body of the text for details. Authors need to spell out upfront and use consistently the various vertical position and direction coordinates utilized, amongst which: receiver height (above reflecting surface), satellite elevation (angle w.r.t. horizon), and altitudes (ellipsoidal and orthometic). Unqualified usage (e.g., "elevation" by itself) is confusing. Also the grazing angle, w.r.t. the surface tangent, needs to be introduced for non-horizontal surfaces, as a generalization of the elevation angle.

➔ Corrections (list not exhaustive):

Page	Line	Before correction	After correction
1	27	With a 50-meter receiver height	50 meters above the reflecting surface
1	29	Altitude up to 2000 m	Orthometric altitude up to 2000 m
1	30	Altitude of 370 m	Orthometric altitude of 370 m
1	52	Increase with the receiver height	Increase with the receiver height above the reflecting surface
3	186	An elevation or azimuthal mask	An elevation or azimuthal angles mask
3	187	To avoid low elevation satellites	To avoid satellites with low elevation angle
3	188	The elevation mask	The elevation angle mask
5	373	Considering the elevation angle of the satellite	Considering the elevation angle of the satellite (considering zenith angle reckoned from the ellipsoidal normal direction)
5	410	The two normalized vectors between the specular reflection point and the transmitter, and the specular reflection point and the receiver	The two normalized anti-incident and scattering vectors.
5	411	The sum of the two vectors	The bisecting vector
7	554	We thus obtain the corrected elevation of the incoming wave	We thus obtain the corrected incident angle of the incident wave
7	556	The corrected elevation	The corrected incident angle
8	681	Of the satellite elevation	Of the satellite elevation angle

8	682	The receiver height	The receiver height above the reflecting surface
8	687	An important receiver height	A big receiver height above the reflecting surface
8	696	The receiver height	The receiver height above the sea surface
8	699	For low elevation satellites	For satellites with low elevation angles
9	730	Influence of the receiver height	Influence of the receiver height above the reflecting surface
9	732	Increase with the receiver height	Increase with the receiver height above the reflecting surface
9	754	Satellite elevations	Satellites elevation angles
9	757	Satellite elevation	Satellites elevation angle
9	760	Whose elevation is between	Whose elevation angle is between
9	762	The lower the satellite elevation is	The lower the satellite elevation angle is
9	805	i.e. for low satellite elevations and high receiver height	i.e. for low satellite elevation angles and high receiver height above the reflecting surface
10	816	And with satellite elevation above 5°	And with satellite elevation angle above 5°
10	821	To the receiver height	To the receiver height above the reflecting surface
10	824	A big receiver height	A big receiver height above the reflecting surface
10	825	For the same elevation	For the same elevation angle
10	832	For low satellite elevation	Low satellite elevation angle
10	836	Satellites elevation inferior to 10°	Satellites elevation angle lower than 10°

The original SRTM was provided as orthometric heights w.r.t. the older EMG96 geoid. Using geoidal undulations from the newer EGM08 would be inconsistent with the way SRTM was generated. Please check.

➔ You are right. I corrected it by using a EGM96 grid instead of the EGM08 and simulations have been recomputed. See subsection 2.4 Earth Gravitational Model EGM96, page 3, line 204.

2.4 Earth Gravitational Model EGM96

In order to be able to convert between ellipsoidal heights (with respect to the WGS84 ellipsoid) and altitudes (with respect to the EGM96 geoid model) when producing KML files or when integrating a DEM, the knowledge of the geoid undulation is mandatory. In this study, we interpolate a 15 x 15-Minute Geoid Undulation Grid file derived from EGM96 model in a tide-free system released by the U.S. National Geospatial-Intelligence Agency (NGA) EGM Development Team: http://earth-info.nga.mil/GandG/wgs84/gravitymod/. The error on the interpolation is lower than 2 cm (NASA and NIMA , 1998).

The Gaussian radius of curvature should be preferred over the meridional radius of curvature used. I believe the spherical approximation is osculating rather than geocentric as stated in the text; this is a consequence of the type of elevation angle employed, whose complement is reckoned from the ellipsoidal normal direction rather than the geocentric radial direction.

➔ Corrected, in particular in page 5, line 368:

$$r_E = \frac{a^2 b}{a\cos(\varphi)^2 + b\sin(\varphi)^2}$$

With *the Gaussian radius of curvature at the latitude of the receiver* φ_r

---

Glistening zone and Fresnel zone are confounded in the text.
Formulas given for first Fresnel zone are not valid for near-surface receivers.

➔ Corrected. Figure 15 showing the first Fresnel zones with respect to the receiver height above reflecting surface and satellite elevation angle has been re-done taking the correct formulas (w.r.t. the receiver height). See subsection 3.6 Footprint size of the reflected signal, page 7, line 585.

3.6 Footprint size of the reflected signal

The signal power received is mostly due to coherent reflection and most of scattering is coming from the first Fresnel zone (Beckmann P. and Spizzichino A. , 1987). The first Fresnel zone can be described as an ellipse of semi-minor axis (a) and semi-major axis (b) equal to (Larson K.M. and Nievinski F.G. , 2013):

$$r_b = \sqrt{\frac{\lambda h}{sin(\epsilon')} + (\frac{\lambda}{2sin(\epsilon')})^2} \qquad (20)$$

$$r_a = \frac{b}{sin(\epsilon')} \qquad (21)$$

With λ the wave length (m), h the receiver height (m) and ε' the satellite elevation seen from the specular reflection point (rad) (i.e. corresponds to the reflection angle).

TECHNICAL CORRECTIONS

Please see annotated PDF.

➔ Corrections, particularly (list not exhaustive):

Page	Line	Before correction	After correction
1	1	Simulations of direct and reflected waves trajectories for in situ GNSS-R experiments	Simulations of direct and reflected waves trajectories for ground-based GNSS-R experiments
1	25	The first one at the top of the Cordouan lighthouse (45°35'11"N ; 1°10"24"W ; 65 m) and the second one in the shore of the Geneva lake (46°24'30"N ; 6°43'6"E, with a 50-meter receiver height)	The first one at the top of the 65 meters Cordouan lighthouse in the Gironde estuary, France, and the second one in the shore of the Geneva lake
1	61	Fresnel first surfaces	First Fresnel zones
1	62	For a convenient use	For visualizing with Google Earth
2	95	On-board aircraft antennas	Airborne antennas
2	118	These reflected waves will change their polarization from RHCP to LHCP by reflecting.	These reflected waves will mostly change their polarization from RHCP to LHCP by reflecting at near-normal incidence.
3	181	These products are available on the IGS website.	Ephemeris products are available on the IGS website (…) and Keplerian parameters e.g. on (…).
3	189	The elevation mask commonly used is set to (10°;90°)	The elevation angle mask commonly used is set to 10° min and 90° max
3	256	Especially	especially
3	260	Data used for validation	Data used for assessment
4	277	Simple difference	Single difference
4	353		WGS84 has Z polar and X,Y equatorial
5	406	Local ellipsoid approximation	Ellipsoid reflection approximation
6	525	To the ground	To the surface
6	525	From the ground	From the surface
7	541	Satellite-ground path	Satellite-surface path

7	558	The ground-receiver path	The surface-receiver path
10	886	Inferior to	Smaller than
10	888	Superior to	Greater than

As suggested, some references have been added:

- Beckmann P., Spizzichino A.: Scattering of Electromagnetic Waves from Rough Surfaces. Artech House Publishers. 1987. ISBN 0-89006-238-2.
- Kostelecky J., Klokocnik J., Wagner C.A.: Geometry and accuracy of reflecting points in bistatic satellite altimetry. J Geod (2005) 79: 421-430. DOI: 10.1007/s00190-005-0485-7, 2005.
- Lagler K., Schindelegger M., Boehm J., Krsn H., Nilsson T. GPT2: Empirical slant delay model for radio space geodetic techniques. Geophysical Research Letters 40(6):1069–1073, doi:10.1002/grl.50288. 2013.
- Larson K.M., Nievinski F.G.: GPS snow sensing: results from the EarthScope Plate Boundary Observatory. GPS Solut. 17:41-52, DOI 10.1007/s10291-012-0259-7, 2013.
- NASA and NIMA: The Development of the Joint NASA GSFC and the National Imagery and Mapping Agency (NIMA) Geopotential Model EGM96. NASA/TP-1998-206861. 1998.
- Nievinski F.G.: Ray-tracing options to mitigate the neutral atmosphere delay in GPS, thesis (Ph.D.), 255 p., 2009.
- Wagner C., Klokocnik C.: The value of ocean reflections of GPS signals to enhance satellite altimetry: data distribution and error analysis. Journal of Geodesy (2003) 77: 128-138. DOI: 10.1007/s00190-002-0307-0, 2003.

And some references have been removed:

- Ferrazzoli P., Guerriero L., Pierdicca N., Rahmoune R.: Forest biomass monitoring with GNSS-R: Theoretical simulations. ADV SPACE RES, Vol. 47, 1823-1832, DOI: 10.1016/j.asr.2010.04.025, 2010.
- Park H., Marchan-Hernandez J.F., Rodriguez-Alvarez N., Valencia E., Ramos-Perez I., Bosch-Lluis X., Camps A.: End-to-end Simulator for Global Navigation Satellite System Reflectometry Space Mission. IEEE International Geoscience and Remote Sensing Symposium IGARSS 2010, Honolulu, Hawaii, USA, 2010.
- Pavlis N.K., Holmes S.A., Kenyon S., Factor J.K.: The Development and Evaluation of the Earth Gravitational Model 2008 (EGM2008). J. Geophys. Res., doi:10.1029/2011JB008916,2012.
- Beckmann P., Spizzichino A.: Scattering of Electromagnetic Waves from Rough Surfaces. Artech House Publishers. 1987. ISBN 0-89006-238-2.

As suggested, some figures have been removed, and more text have been added under them in order to help the reader to understand the figures. Hereafter are the remaining figures with the new captions.

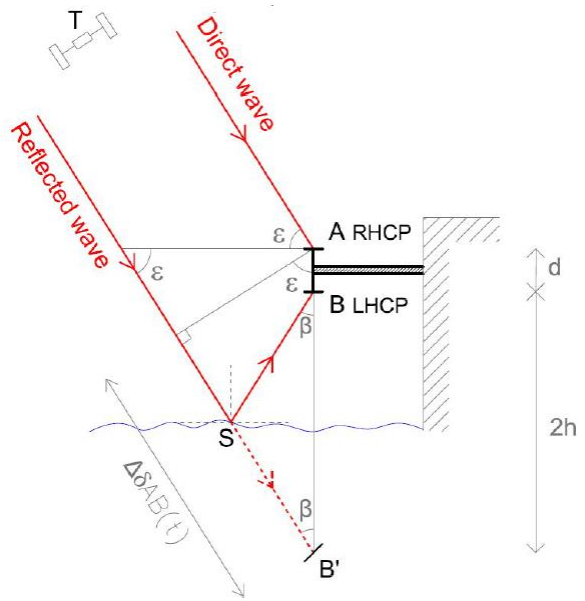

Fig. 1. Principle of GNSS-Reflectometry.
T: satellite/transmitter, S: specular reflection point, ϵ: satellite elevation, $\triangle\ \delta AB(t)$: additional path covered by the reflected wave, d : interdistance between the LHCP and RHCP antennas and h: height of the receiver above the reflecting surface.

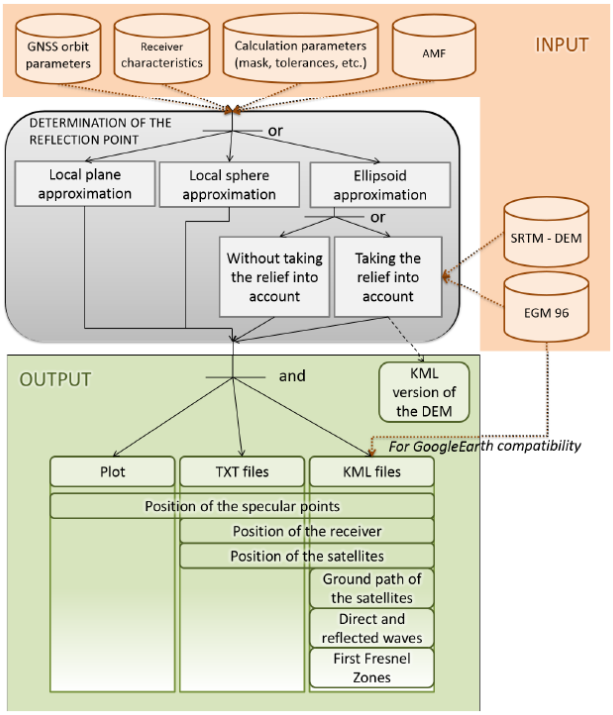

Fig. 2. Data flow chart of the simulator.
Three main blocks: an input block which contains the different elements mandatory for the processing; a processing block where the user can choose which algorithm to be used, and an output block containing the different results of the simulation, namely KML files to be opened with Google Earth.

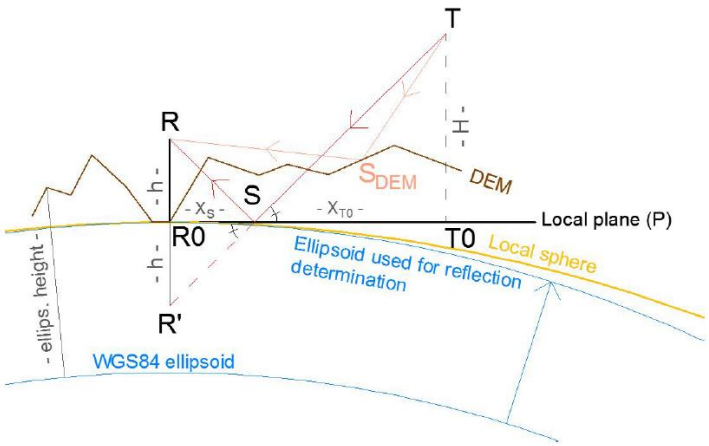

Fig. 1. Determination of the specular reflection point in a local plane approximation and local difference with the sphere and ellipsoid approximations and DEM integration.
S: specular reflection point position. R: receiver position. T: transmitter/satellite position. h: height of the receiver above the ground surface.

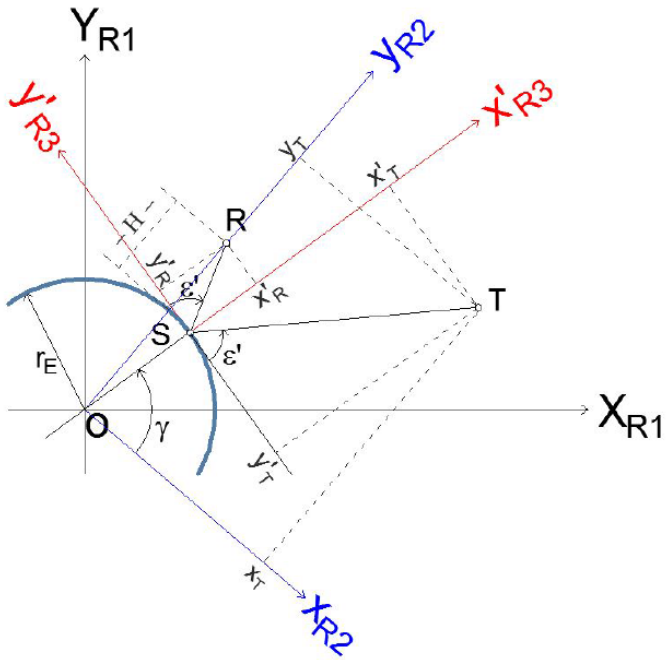

Fig. 4. Local sphere approximation : the three different reference systems of coordinates.

S: specular reflection point position. R: receiver position. T: transmitter/satellite position. $(0, X, Y, Z)_{R1}$: WGS84 Cartesian system. $(0, x, y)_{R2}$: local two-dimensional system, obtained by the rotation of the R1 system around the Z axis, in such a way that $x_r = 0$.$(S, x', y')_{R3}$: a local two-dimensional system, obtained by a rotation around the z axis and a r_R translation of the R2 system in such a way that x' and the local vertical are colinear and that the system origin coincides with the specular reflection point S.

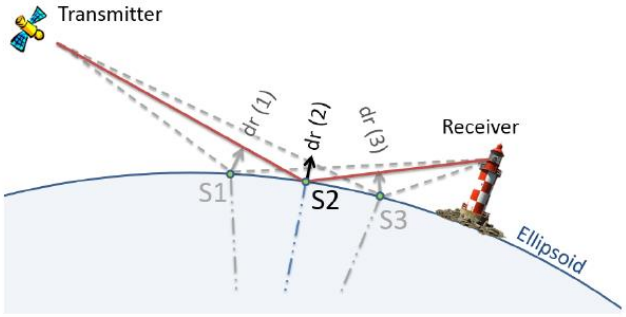

Fig. 5. Local ellipsoid approximation.

S2: specular reflection point position. S1, S3: temporary positions of the specular reflection point before convergence. Let dr be the sum of the normalized anti-incident and scattering vector (i.e. the bisecting vector). In the specular reflection point position, dr is colinear with the local vertical. We apply a dichotomous process until having this condition verified.

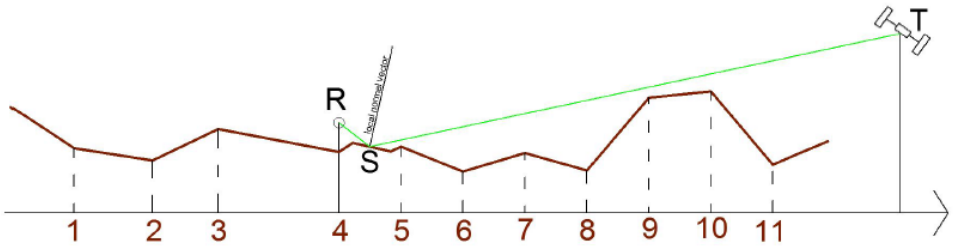

Fig. 6. Determination of the specular reflection point integrating a DEM
S: specular reflection point position. R: receiver position. T: transmitter/satellite position. A dichotomous process is applied for each topographic segment of the DEM to find if there is a point where the bisecting angle (equal to the sum of the anti-incident and scattering vectors) is colinear with the local normal vector.

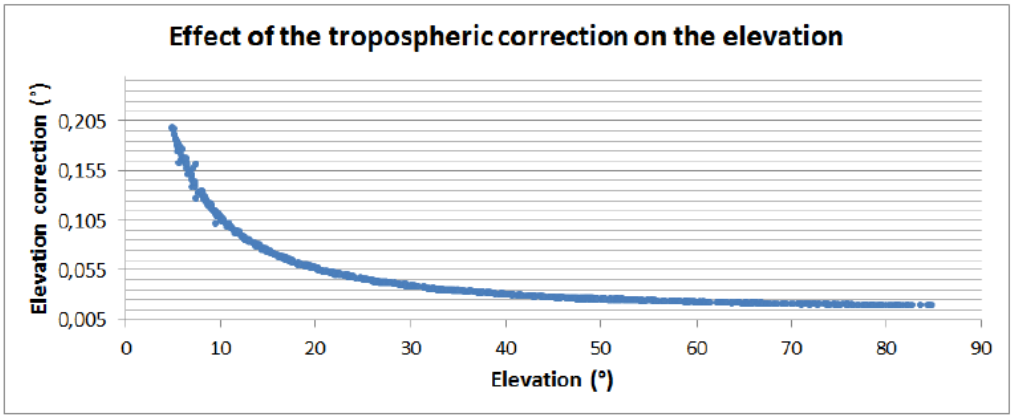

Fig. 7. Effect of the neutral atmosphere on the elevation angle.
An exponential correction must be made for satellites with low elevation angle.

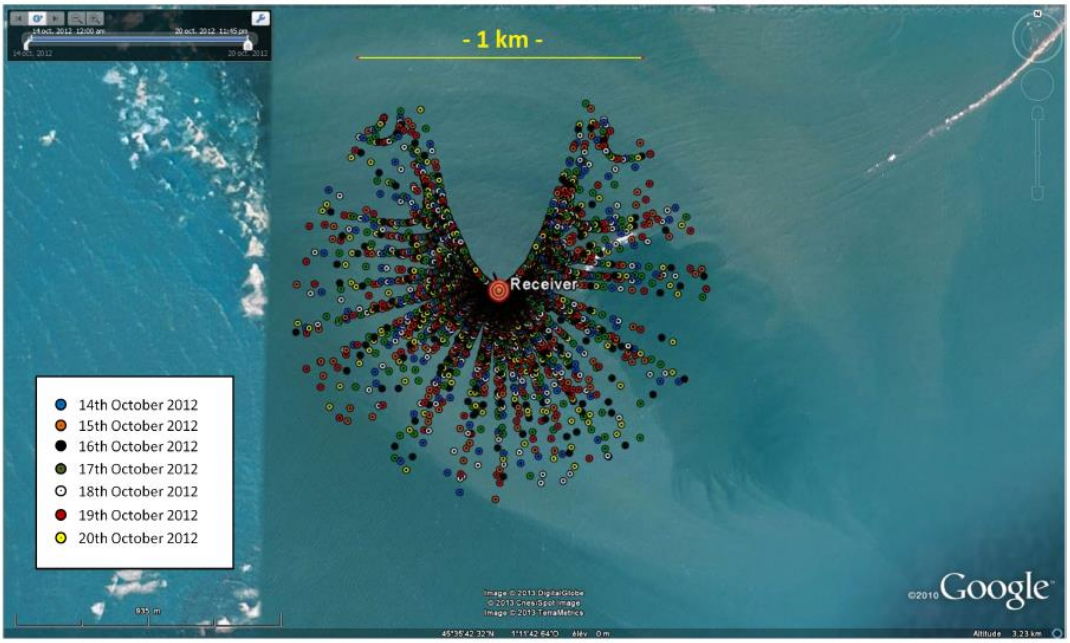

Fig. 8. Positions of the specular reflection points for one week of simulation on the Cordouan lighthouse with a 15 minutes sampling rate (i.e. satellites positions actualized each 15 minutes).
Note the gap in the North direction.

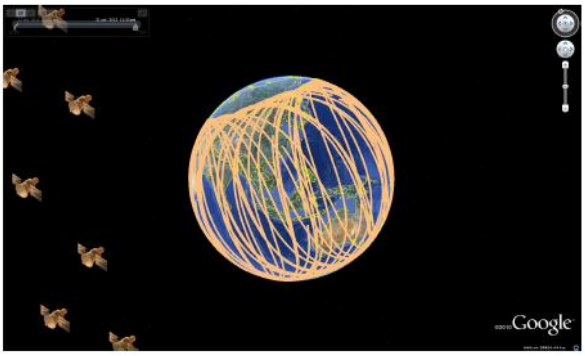

Fig. 9. Ground tracks of the GPS satellites the 4^{th} October 2012.

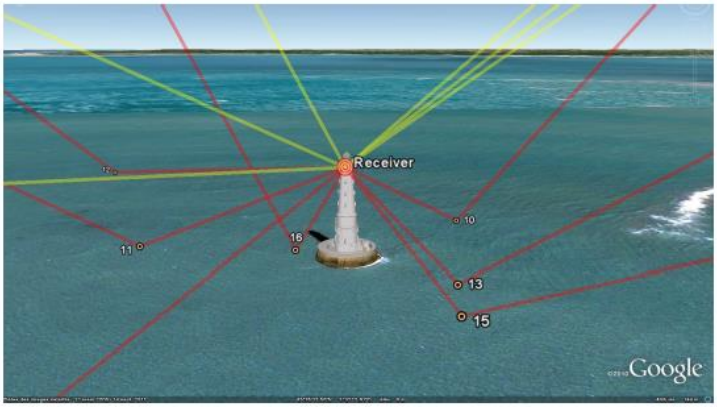

Fig. 10. Direct and reflected waves display: Cordouan lighthouse simulation.

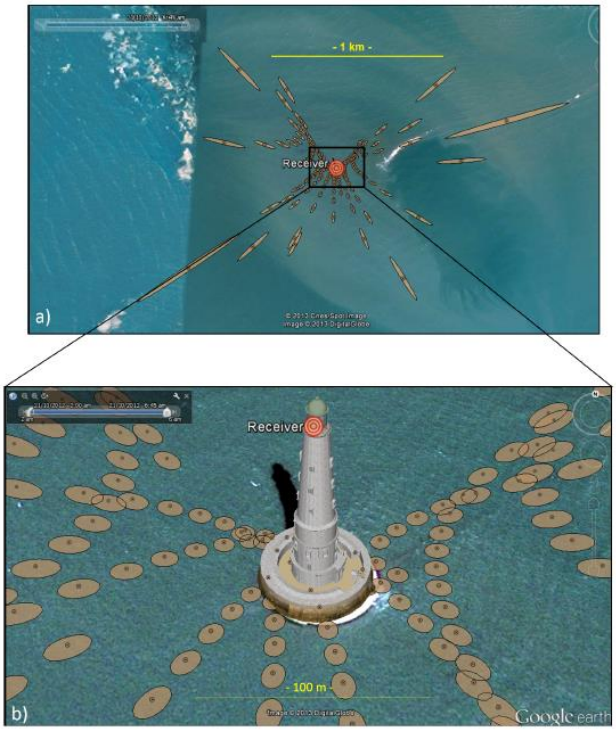

Fig. 11. First Fresnel surfaces distribution
a) global point of view with a radius close to 1 km; b) zoom centered on the Cordouan lighthouse.

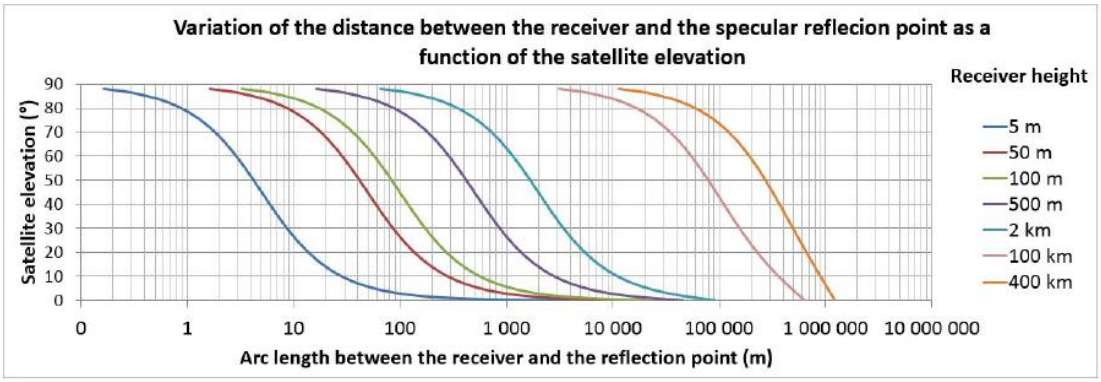

Fig. 12. Variation of the distance between the receiver and the specular reflection point, as a function of the satellite elevation, for different receiver heights.

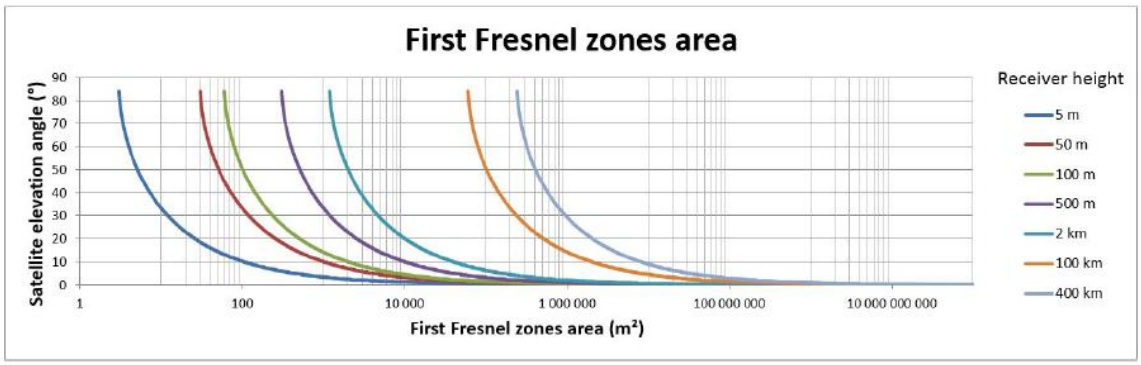

Fig. 13. First Fresnel surface area as a function of the satellite elevation, for different receiver heights.

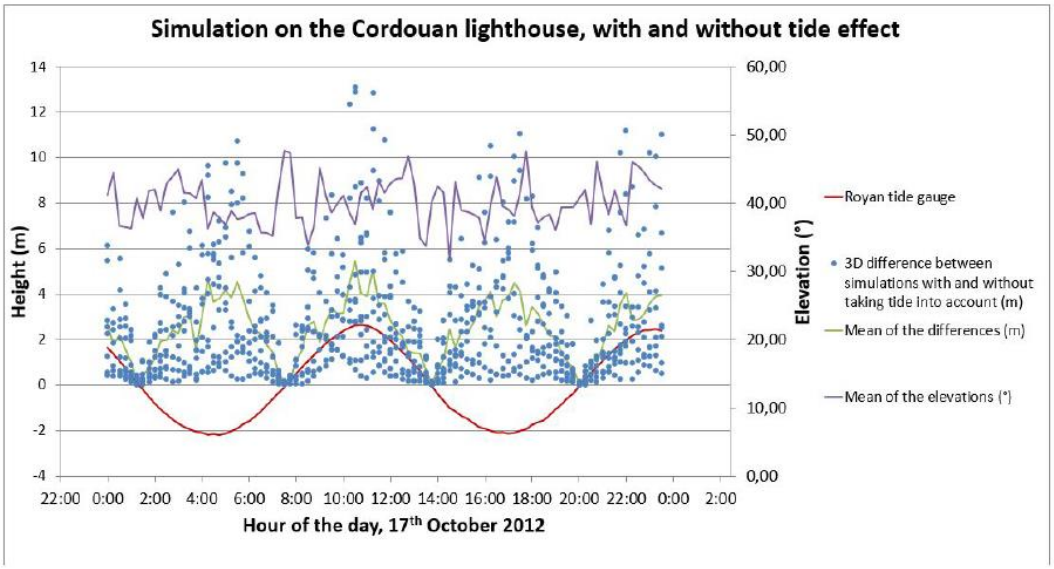

Fig. 14. Assessment of the tide influence.
The red line shows the tide from the Royan tide gauge and must be linked with the left vertical axis. The blue dots (resp. green line) are the 3D differences (resp. mean of the 3D differences) between simulations with and without taking the tide into account (i.e. taking the mean sea level over the period as reference) and must also be read with the left vertical axis. The purple line must be read with the right vertical axis and shows the mean of the satellite elevation angles. The impact of the tide on the size of the reflecting area is non-negligible (decametric 3D-differences), and it is worth noticing that the gaps would have been even bigger integrating satellites with low elevation angle. Note also the fact that the periodic variations of the 3D variations are only linked to the tide, since the mean of the satellite elevation angles does not show periodic variation during the day of simulation.

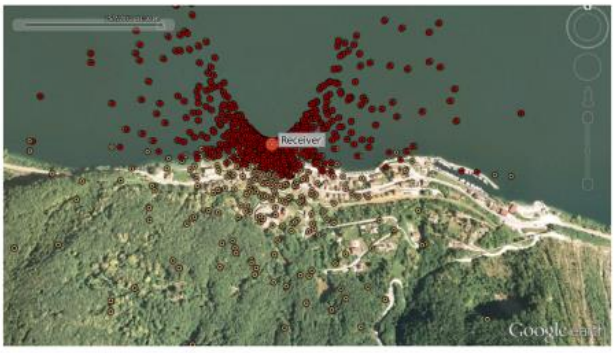

Fig. 15a. Influence of the relief - Specular reflection points on the shore of the Geneva lake (46°24'30N";6°43'6"E).
Red dots: sphere approximation algorithm (altitudes have been increased so that all the points be visible) Orange dots: taking a DEM into account

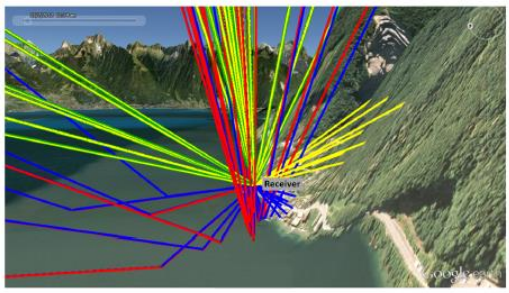

Fig. 15b. Influence of the relief - Direct and reflected waves display. (Relief amplifier by a factor 3) Yellow lines: direct waves, sphere approximation algorithm ; Green lines: direct waves, taking a DEM into account ; Blue lines: reflected waves, sphere approximation algorithm ; Red lines: reflected waves, taking a DEM into account. It is noticeable that some yellow and blue lines (direct and reflected waves, sphere approximation algorithm) go through the moutain (reflection points having been calculated *inside* the moutain), whereas any red or green line (direct and reflected waves, intergrating a DEM) go through it.

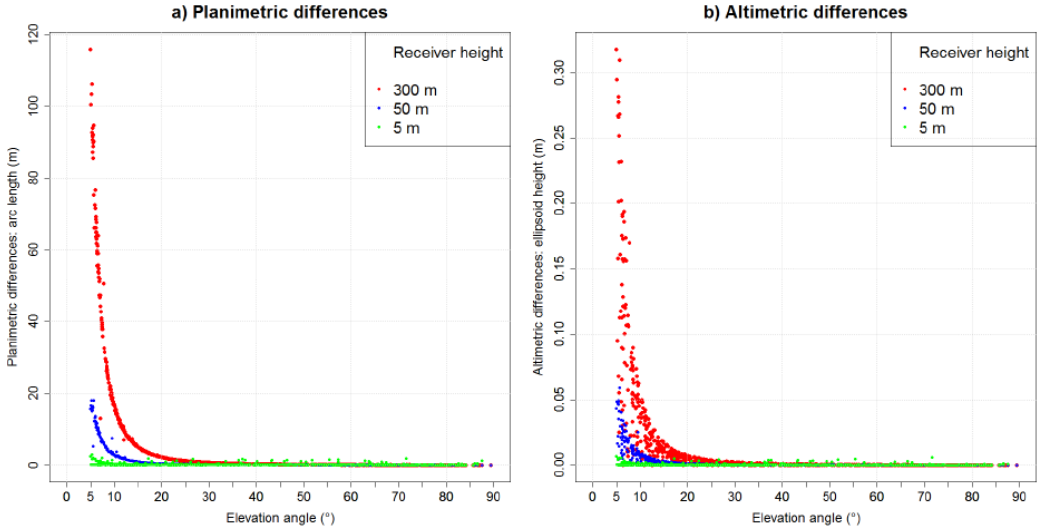

Fig. 16. Importance of tropospheric correction versus elevation and receiver height with respect to reflecting surface height. a) Planimetric differences as arc length (m). b) Altimetric differences as ellipsoid height (m).

Table 2. Position differences (arc length and 3D geometric distance) between the different algorithms. Height: 5 m, elevation > 5°.

Vertical visibility mask (°)		**5 - 90**					
Horizontal visibility mask (°)		0 - 360					
Receiver height (m)		**5**					
Algorithm		Sphere	Plane	Sphere	Ellipsoid	Sphere	DEM
Distance with respect to the receiver: arc length (m)	Minimum	0.23	0.23	0.23	0.23	0.23	0.21
	Maximum	57.32	57.33	57.32	55.56	57.32	66.98
	Mean	11.30	11.30	11.30	11.26	11.30	12.95
	Standard deviation	11.59	11.59	11.59	11.47	11.59	13.65
Propagation difference (m)	Minimum	0.87	0.87	0.87	0.87	0.87	0.00
	Maximum	9.99	9.99	9.99	9.99	9.99	0.59
	Mean	5.68	5.69	5.68	5.68	5.68	0.13
	Standard deviation	2.81	2.81	2.81	2.81	2.81	0.12
Planimetric differences (m) (cartesian WGS84 / geodesic arc-length)	Minimum	0.00/0.00		0.02 / 0.00		3.12 / 0.00	
	Maximum	0.01 / 0.00		1.44 / 1.81		22.96 / 20.94	
	Mean	**0.00 / 0.00**		**0.10 / 0.11**		**6.67 / 2.25**	
	Standard deviation	0.00 / 0.00		0.19 / 0.25		1.57 / 1.99	
Altimetric differences (m) (cartesian WGS84 / geodesic arc-length)	Minimum	0.00/0.00		0.02 / 0.00		4.84 / 8.74	
	Maximum	0.01 / 0.01		1.24 / 0.17		10.29 / 10.86	
	Mean	**0.00 / 0.00**		**0.08 / 0.02**		**6.82 / 9.22**	
	Standard deviation	0.00 / 0.00		0.15 / 0.03		0.92 / 0.41	

Table 3. Position differences (arc length and 3D geometric distance) between the different algorithms. Height: 50 m, elevation > 5°.

Vertical visibility mask (°)		**5 - 90**					
Horizontal visibility mask (°)		0 - 360					
Receiver height (m)		**50**					
Algorithm		Sphere	Plane	Sphere	Ellipsoid	Sphere	DEM
Distance with respect to the receiver: arc length (m)	Minimum	2.21	2.21	2.21	2.05	2.21	0.19
	Maximum	572.38	573.28	572.38	554.84	572.38	6678.56
	Mean	104.32	104.36	104.32	103.66	104.32	527.53
	Standard deviation	111.69	111.79	111.69	109.91	111.69	553.92
Propagation difference (m)	Minimum	8.67	8.66	8.67	8.94	8.67	102.09
	Maximum	99.91	99.91	99.91	99.92	99.91	763.27
	Mean	59.44	59.44	59.44	59.46	59.44	368.01
	Standard deviation	27.80	27.80	27.80	27.75	27.80	149.11
Planimetric differences (m) (cartesian WGS84 / geodesic arc-length)	Minimum	0.00/0.00		0.22 / 0.31		7.02 / 1.87	
	Maximum	0.73 / 1.06		13.51 / 17.99		5391.80 / 5443.61	
	Mean	**0.03 / 0.06**		**0.92 / 1.20**		**101.29 / 90.95**	
	Standard deviation	0.10 / 0.15		1.76 / 2.29		379.44 / 375.87	
Altimetric differences (m) (cartesian WGS84 / geodesic arc-length)	Minimum	0.00/0.00		0.17 / 0.00		0.03 / 4.19	
	Maximum	0.53 / 0.03		12.32 / 1.64		953.09 / 1053.38	
	Mean	**0.02 / 0.00**		**0.77 / 0.19**		**19.28 / 40.07**	
	Standard deviation	0.06 / 0.00		1.51 / 0.27		81.44 / 93.69	

Table 4. Position differences (arc length and 3D geometric distance) between the different algorithms. Height: 300 m, elevation > 5°.

Vertical visibility mask (°)		**5 - 90**					
Horizontal visibility mask (°)		0 - 360					
Receiver height (m)		**300**					
Algorithm		Sphere	Plane	Sphere	Ellipsoid	Sphere	DEM
Distance with respect to the receiver: arc length (m)	Minimum	13.26	13.26	13.26	12.32	13.26	0.19
	Maximum	3407.44	3439.29	3407.44	3304.53	3407.44	6678.57
	Mean	660.75	662.36	660.75	656.16	660.75	733.13
	Standard deviation	714.13	717.99	714.13	703.71	714.13	810.51
Propagation difference (m)	Minimum	52.15	51.99	52.15	53.78	52.15	11.88
	Maximum	599.45	599.45	599.45	599.49	599.45	763.28
	Mean	353.16	353.13	353.16	353.40	353.16	335.48
	Standard deviation	172.72	172.75	172.72	172.43	172.72	168.19
Planimetric differences (m) (cartesian WGS84 / geodesic arc-length)	Minimum	0.00/0.00		1.33 / 1.95		7.02 / 1.87	
	Maximum	25.98 / 37.56		79.18 / 105.64		5391.80 / 5443.61	
	Mean	**1.42 / 2.05**		**5.86 / 7.70**		**100.51 / 91.84**	
	Standard deviation	3.88 / 5.62		10.95 / 14.26		378.05 / 375.10	
Altimetric differences (m) (cartesian WGS84 / geodesic arc-length)	Minimum	0.00/0.00		1.02 / 0.00		0.03 / 0.33	
	Maximum	18.70 / 1.02		72.46 / 9.79		953.09 / 1053.38	
	Mean	**0.68 / 0.08**		**5.02 / 1.19**		**20.36 / 36.70**	
	Standard deviation	2.20 / 0.16		9.43 / 1.68		79.98 / 89.66	

Table 5. Position differences (arc length and 3D geometric distance) between the different algorithms. Height: 5 m, elevation > 10°.

Vertical visibility mask (°)		**10 - 90**					
Horizontal visibility mask (°)		0 - 360					
Receiver height (m)		**5**					
Algorithm		Sphere	Plane	Sphere	Ellipsoid	Sphere	DEM
Distance with respect to the receiver: arc length (m)	Minimum	0.23	0.23	0.23	0.23	0.23	0.21
	Maximum	27.74	27.75	27.74	27.55	27.74	37.18
	Mean	8.22	8.22	8.22	8.23	8.22	9.12
	Standard deviation	6.54	6.54	6.54	6.53	6.54	7.45
Propagation difference (m)	Minimum	1.77	1.77	1.77	1.78	1.77	0.00
	Maximum	9.99	9.99	9.99	9.99	9.99	0.59
	Mean	6.15	6.15	6.15	6.15	6.15	0.14
	Standard deviation	2.54	2.54	2.54	2.54	2.54	0.12
Planimetric differences (m) (cartesian WGS84 / geodesic arc-length)	Minimum	0.00/0.00		0.02 / 0.00		4.36 / 0.00	
	Maximum	0.01 / 0.00		0.41 / 0.48		12.94 / 10.03	
	Mean	**0.00 / 0.00**		**0.06 / 0.05**		**6.70 / 1.80**	
	Standard deviation	0.00 / 0.00		0.05 / 0.08		1.26 / 1.35	
Altimetric differences (m) (cartesian WGS84 / geodesic arc-length)	Minimum	0.00/0.00		0.02 / 0.00		4.91 / 8.91	
	Maximum	0.01 / 0.01		0.33 / 0.09		8.78 / 10.86	
	Mean	**0.00 / 0.00**		**0.04 / 0.01**		**6.62 / 9.25**	
	Standard deviation	0.00 / 0.00		0.04 / 0.02		0.65 / 0.42	

Table 6. Position differences (arc length and 3D geometric distance) between the different algorithms. Height: 50 m, elevation > 10°.

Vertical visibility mask (°)		**10 - 90**					
Horizontal visibility mask (°)		0 - 360					
Receiver height (m)		**50**					
Algorithm		Sphere	Plane	Sphere	Ellipsoid	Sphere	DEM
Distance with respect to the receiver: arc length (m)	Minimum	2.21	2.21	2.21	2.05	2.21	0.19
	Maximum	277.34	277.44	277.34	275.42	277.34	6678.56
	Mean	76.38	76.38	76.38	76.27	76.38	527.53
	Standard deviation	63.09	63.10	63.09	62.83	63.09	553.92
Propagation difference (m)	Minimum	17.66	17.66	17.66	17.78	16.66	102.09
	Maximum	99.91	99.91	99.91	99.92	99.91	763.27
	Mean	63.85	63.85	63.85	63.5	63.85	368.01
	Standard deviation	24.91	24.91	24.91	24.88	24.91	149.11
Planimetric differences (m) (cartesian WGS84 / geodesic arc-length)	Minimum	0.00/0.00		0.22 / 0.31		7.02 / 1.87	
	Maximum	0.10 / 0.16		4.08 / 4.79		5391.80 / 5443.61	
	Mean	**0.01 / 0.02**		**0.48 / 0.64**		**101.29 / 90.95**	
	Standard deviation	0.02 / 0.04		0.46 / 0.58		379.44 / 375.87	
Altimetric differences (m) (cartesian WGS84 / geodesic arc-length)	Minimum	0.00/0.00		0.17 / 0.00		0.03 / 4.19	
	Maximum	0.06 / 0.01		3.27 / 0.86		953.09 / 1053.38	
	Mean	**0.00 / 0.00**		**0.42 / 0.13**		**19.28 / 40.07**	
	Standard deviation	0.01 / 0.00		0.40 / 0.14		81.44 / 93.69	

Table 7. Position differences (arc length and 3D geometric distance) between the different algorithms. Height: 300 m, elevation > 10°.

Vertical visibility mask (°)		**10 - 90**					
Horizontal visibility mask (°)		0 - 360					
Receiver height (m)		**300**					
Algorithm		Sphere	Plane	Sphere	Ellipsoid	Sphere	DEM
Distance with respect to the receiver: arc length (m)	Minimum	13.26	13.26	13.26	12.32	13.26	0.19
	Maximum	1660.78	1664.57	1660.78	1649.33	1660.78	6678.56
	Mean	453.50	453.83	453.50	452.28	453.50	527.53
	Standard deviation	381.89	382.46	381.89	379.68	381.89	553.92
Propagation difference (m)	Minimum	106.02	105.94	106.02	105.94	106.02	102.09
	Maximum	599.45	599.45	599.45	599.49	599.45	763.27
	Mean	386.56	386.54	386.56	386.71	386.56	368.01
	Standard deviation	152.00	152.02	152.00	151.81	152.00	149.11
Planimetric differences (m) (cartesian WGS84 / geodesic arc-length)	Minimum	0.00/0.00		1.34 / 1.95		7.02 / 1.87	
	Maximum	3.66 / 5.32		18.02 / 26.10		5391.80 / 5443.61	
	Mean	**0.30 / 0.43**		**2.80 / 3.81**		**101.29 / 90.95**	
	Standard deviation	0.59 / 0.86		2.51 / 3.31		379.44 / 375.87	
Altimetric differences (m) (cartesian WGS84 / geodesic arc-length)	Minimum	0.00/0.00		1.02 / 0.00		0.03 / 4.19	
	Maximum	2.22 / 0.23		19.51 / 4.57		953.09 / 1053.38	
	Mean	**0.12 / 0.03**		**2.61 / 0.75**		**19.28 / 40.07**	
	Standard deviation	0.26 / 0.04		2.41 / 0.80		81.44 / 93.69	

Geosci. Model Dev. Discuss., 7, C132–C138, 2014
www.geosci-model-dev-discuss.net/7/C132/2014/

Open Access
Geoscientific Model Development

Interactive comment on "Simulations of direct and reflected waves trajectories for in situ GNSS-R experiments" by N. Roussel et al.

Received and published: 02 May 2014

➔ Following the main point of the first reviewer, many new calculations were done, and the text of the article was supplemented by new results. As attachment you will find the modified version of the article (RousselN_new.pdf) and also a pdf file where modifications and corrections between the two versions of the article are highlighted (RousselN_corrections.pdf).

SUMMARY

The authors have developed a simulator to determine the locations of surface reflection points by modeling the transmissions from GNSS satellites. They investigate multiple approaches to modeling Earth's surface, including a digital elevation model (with potential obscuration) and incorporate a troposphere model. The latter is shown to have significant impact.
The work appears to be a very useful tool. However, some of the results are puzzling.
Some assumptions are not fully worked out. In addition, no validations are performed against prior work. These issues must be addressed prior to publication.

➔ Cross-comparisons have been performed between the algorithms approximating the Earth as a sphere or as an ellipsoid and between the algorithm approximating the Earth as an ellipsoid and the one integrating a DEM in a new subsection 4.2 *Validation of the surface models*, page 7, line 611.
The one with the ellipsoid approximation is based on an iterative scheme, while the one with the sphere approximation is based on an analytical determination. Differences between both of them are sub millimetric when putting the semi-major and minor axis of the ellipsoid equal to the Earth radius.

4.2 Validation of the surface models

Simulations have been performed in the case of the Geneva Lake shore, for a 24-hour experiment, on the 4th October 2012.

4.2.1 Cross-validation between sphere and ellipsoid approximations

Local sphere and ellipsoid approximation algorithms have been compared by putting the ellipsoid semi-major and minor axis equal to the sphere radius. Planimetric and altimetric differences between both are below 6.10^{-5} m for a receiver height above reflecting surface between 5 and 300 m and are then negligible. The two algorithms we compare are totally different: the first is analytical and the second is based on a iterative scheme and both results are very similar, which confirms their validity.

4.2.2 Cross-validation between ellipsoid approximation and DEM integration

The algorithm integrating a DEM has been compared to the ellipsoid approximation algorithm by putting a flat DEM as input (i.e. a DEM with orthometric altitude equal to the geoid undulation). Results for satellite elevation angles above 5° are presented in table 1. As we can see in table 1, planimetric and altimetric mean differences are subcentimetric for a 5 and 50 m receiver height and centimetric for a 300 m receiver height. However, some punctual planimetric differences reach 70 cm in the worst conditions (reflection occurring at 3408 m from the receiver corresponding to a satellite with a low elevation angle), which can be explained with the chosen tolerance parameters but mainly because due to the DEM resolution, the algorithm taking a DEM into account approximating the ellipsoid as a broken straight line, causing inaccuracies. For a 50 m receiver height, planimetric differences are below 10 cm (reflections occurring until 573 meters from the receiver). With regards to the altimetric differences, even for reflections occurring far from the receiver, the differences are negligible (submillimetric).

Table 1. Cross-validation between ellipsoid approximation and DEM integration

		Receiver height (m)		
		5	50	300
Distance to the specular reflection point with respect to the receiver: arc length (m)	Mean	13	122	730
	Maximum	58	573	3408
Position differences (m) (planimetric / altimetric)	Mean	**0.007/0**	**0.008/0**	**0.04/0**
	Maximum	0.1/0	0.1/0	0.7/0

DETAILED COMMENTS

Abstract: “DEM” is used before it is defined

➔ Corrected → page 1, line 43.

p.1009, Line 23 (1009-23): This assumption is not justified, particular when a DEM is used. The authors should at least justify this assumption and have some quantitative estimate as to the error made by this assumption, and understand the implications of this assumption.

➔ Indeed, this assumption is only relevant for the local plane, sphere or ellipsoid approximation and not when integrating a DEM.
In the plane, sphere and ellipsoid approximations, the specular reflection point of a given satellite is contained within the plane defined by the satellite, the receiver and the center of the Earth. With regards to the DEM integration, reflection can occur everywhere, but I only consider those contained in the plane: first because considering all the potential reflections would take a huge calculation time, and secondly because I consider the DEM integration as a way to have positions closer to reality w.r.t the sphere, plane or ellipsoid approximations, i.e. as a correction to the other algorithms, where reflections occur only within the plane.
Please see subsection 3.4 Ellipsoid reflection approximation combined with a DEM, page 6, line 440.

3.4 Ellipsoid reflection approximation combined with a DEM

The two first approaches presented above are well adapted in the case of an isolated receiver, located on the top of a light house, for instance. In most of the cases, the receiver is located on a cliff, a sand dune, or a building overhanging the sea surface or a lake. It can however be really appropriate and necessary to incorporate a Digital Elevation Model (DEM) into the simulations, in order not to only take the mask effects (e.g., a mountain occulting a GNSS satellite) into account, but also to get more accurate and realistic positions of specular reflection points. The method we propose here consists of three steps later detailed in subsections 3.4.1, 3.4.2 and 3.4.3.

1. A ”visibility” determination approach to determine if the receiver is in sight of each GNSS satellite.

2. A determination of the specular reflection point position.

3. A ”visibility” determination approach to determine if the determined specular point is in plane of sight receiver/satellite.

We have to keep in mind that a DEM gives altitudes above a reference geoid. For consistency purpose, the positions of the receiver and the transmitter, and the DEM grid points have all to be in the same reference system. So it is absolutely mandatory to convert the altitudes of the DEM grid points into ellipsoidal heights by adding the geoid undulation. To do so, a global grid from the EGM96 geoid undulation model with respect to the WGS84 ellipsoid was removed from SRTM DEM grid points.

3.4.1 Visibility of the GNSS satellite from the receiver

This algorithm aims to determine the presence of mask between the receiver and the satellite. The visibility of the satellite and of the receiver, both from the specular point will be checked once the potential specular point position will be found.
Let R, S, and T be the locations of the receiver, the specular point and the satellite/transmitter on the ellipsoid. We interpolate the ellipsoidal heights along the path [TSR] with a step equal to the DEM resolution, with a bivariate cubic or bilinear interpolation. Cubic interpolation is used when 480 *the gradient is big, linear interpolation otherwise. Tests show millimetric differences between cubic and linear interpolation for flat zones but can reach one meter for mountainous areas. We thus obtain a topographic*

profile from R to T. For each segment of this topographic profile, we check if it intersects the path [TR]. If it does, it means that the satellite is not visible from the receiver. If not, we check the next topographic segment, until reaching the end of the path (i.e. T).

3.4.2 Position of the specular point

Once the satellite visibility from the receiver is confirmed, the next step consists in determining the location of the specular reflection point S along the broken line defined as in subsection 3.4.1. In order to simplify the process, we only consider the specular points located into the plane formed by the satellite, the receiver and the center of the Earth. The algorithm is similar to the one used for the ellipsoid approximation and is based on a dichotomous iterative process. The segments formed by the points of the 2D DEM (see figure 6) are all considered susceptible to contain a specular reflection point. For each of this segment, we check the sign of the correction to apply for the two extremities of the segment with the same principle that for the ellipsoid approximation (see subsection 3.3), but with a local vertical component defined as the normal of the considered segment. If the signs are equal, no reflection is possible on this segment. Otherwise, we apply the dichotomous iterative method presented in subsection 3.3 until convergence with respect to the tolerance parameter (fixed to 1e-7°).

3.4.3 Visibility of the determined specular reflection point from the satellite and the receiver

Once the position of the specular reflection point is determined, we check if it is visible from the satellite and the receiver thanks to the algorithm presented in subsection 3.4.1.

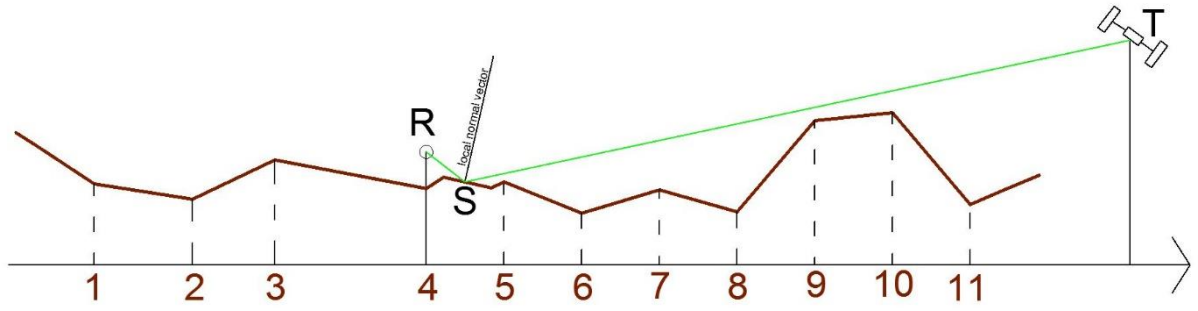

Fig. 6. Determination of the specular reflection point integrating a DEM
S: specular reflection point position. R: receiver position. T: transmitter/satellite position. A dichotomous process is applied for each topographic segment of the DEM to find if there is a point where the bisecting angle (equal to the sum of the anti-incident and scattering vectors) is colinear with the local normal vector.

p. 1015-18: There is something wrong with this sentence.

➔ The sentence has been deleted because a new algorithm has been developed (due to comments from the other referee).

p. 1015-22: Was it not stated earlier that a 2D coordinate system does not always apply? This should be clarified if needed.

➔ The sentence has been deleted because a new algorithm has been developed (due to comments from the other referee).

p. 1021-5: Do not use the word “important” here.

➔ Corrected. Page 8, line 687: “an important receiver height” → “A big receiver height above the reflecting surface”

p. 1023-17: The 8 cm difference seems much too large for the 5 m receiver height, comparing the sphere versus ellipsoid. 8 cm is 0.27% of the maximum reflection point distance from the receiver of 30 m. Distances from the receiver reach up to 30 m for the 5 m altitude antenna. It is hard for me to believe that the difference between sphere and ellipsoid over a 30 m distance approaches 8 cm. 30 m is a small fraction (5x10ˆ-6) of the Earth radius. I do not see how differences of nearly 0.3% are possible over 30 m.
An independent validation or cross check of this code is warranted, to establish there is not an error.

➔ In the new subsection 4.2 *Validation of the surface models,* the spherical model algorithm (analytical with an iterative procedure based on the Newton method to determine the roots of a fourth order polynomial) is compared to the ellipsoid algorithm, which is a pure iterative procedure (close to the algorithm presented in (Kostelechy et al 2005)). By putting the semi-major and –minor axis of the ellipsoid equal to the radius of the sphere, differences are sub-millimetric. The 8 cm difference is the geometric distance between the two determinations of the specular reflection points and is not the difference between the sphere and the ellipsoid.
If the difference between the sphere and the ellipsoid at 30 m is about X cm, the difference between the two determinations of the specular reflection point positions will be far greater than X cm.

4.2.1 Cross-validation between sphere and ellipsoid approximations

Local sphere and ellipsoid approximation algorithms have been compared by putting the ellipsoid semi-major and minor axis equal to the sphere radius. Planimetric and altimetric differences between both are below 6.10^{-5} m for a receiver height above reflecting surface between 5 and 300 m and are then negligible. The two algorithms we compare are totally different: the first is analytical and the second is based on a iterative scheme and both results are very similar, which confirms their validity.

p.1026-5: integration of a DEM must consider the lack of co-planarity is possible between transmitter, receiver and Earth center

➔ You are perfectly right. But same answer as for your first detailed comment. We must precise clearly in the article that we only consider the reflections occurring in the plane defined by the transmitter, the receiver and the Earth center, which is done page 4, line 312.

In the plane, sphere and ellipsoid approximations, the specular reflection point of a given satellite is contained within the plane defined by the satellite, the receiver and the center of the Earth. With regards to the DEM integration, reflection can occur everywhere. In order to be able to compare the specular reflection point positions obtained by integrating a DEM, and to simplify the problem, we will only consider the reflections occurring within the plane, even while integrating a DEM.